DE GRUYTER

Metallurgy

Tanju Teker*, S. Osman Yilmaz and S. Özmen Eruslu

Effect of austempering treatment on metallurgical structure of Ce inoculated X210Cr12 cold work tool steel

Abstract: The effect of austempering treatment on metallurgical structure of X210Cr12 cold work tool steel inoculated with Ce was researched. Microstructural changes, elemental characterizations, and phase formations of the samples were examined by using scanning electron microscopy, energy dispersive spectroscopy, X-ray diffraction, elemental mapping, and microhardness test. Ce inoculation reduced the grain size, and the austenitizing temperature had a huge effect on the austenitizing process. The austenitizing process increased the hardness by reducing the retained austenite, but the degree was dependent on the austenitization temperature. The austempering treatment improved the hardness resistance by depositing more equal carbides composed of nano-sized carbides. High austempering period and increase of austempering temperature decreased the homogeneity and hardness of the microstructure.

Keywords: austempering treatment; cerium inoculation; cold work tool steel; hardness; microstructure.

1 Introduction

Cold work tool steel is ledeburitic steel. It is used in the production of different types of dies, high stress cutting and punching tools, profile rollers, drawing and deep drawing dies, paper and plastic blades, and shear blades for thin sheet metal in sheet molding. Tool steels with various properties are manufactured with suitable alloys to meet the demanding requirements of the industry [1–3].

*Corresponding author: Tanju Teker, Department of Manufacturing Engineering, Faculty of Technology, University of Sivas Cumhuriyet, Sivas, Turkey, E-mail: tanjuteker@cumhuriyet.edu.tr
S. Osman Yilmaz and S. Özmen Eruslu, Department of Mechanical Engineering, Faculty of Engineering, University of Tekirdağ Namık Kemal, Corlu, Tekirdağ, Turkey

Due to the high carbon content and suitable proportions of other alloying elements, quenching can be done without deformation. It is used in press tools where wear and toughness are equally important. Such tool steels are "D" group containing 1.5–2.35 wt% carbon and up to 12 wt% Cr. They are classified according to the quenching medium and alloy composition [4, 5]. In many studies, exceptional elements have been inoculated to develop tool steels. They modify the shape of carbides and are perfectly dispersed in the alloy matrix. The addition of small amounts of specific modifiers to tool steel can alter the eutectic solidification process of the austenite-carbide structure by improving the grain dimension, style, and dispersion of carbides in the matrix [6–8].

The quality of the tool steel can be improved under proper heat treatment. This will vary according to the composition of the alloying elements. Traditional heat treatment consists of quenching, austenitizing, quenching, and tempering. The austenite annealing process converts the remaining austenite to martensite, resulting in a more homogeneous structure. Austenite annealing is a complementary process that can increase wear resistance, dimensional stability, and extend tool life [9–11]. Chen and Li [12] reported that Ti–V–Re added to austempered high silicon steel achieved high fracture toughness when austempered at 350–385 °C with a carbon amount of approximately 1.9–2 wt% and 30–35 wt% retained austenite in austenite.

The aim of this investigation is to examine the effect of austempering treatment on microstructural changes, elemental characterizations, phase formations, and hardness of Ce inoculated cold work tool steel.

2 Materials and methods

The chemical composition of the steel used for experimental research is identified in Table 1. First, the alloy was melted in a 300 kg induction furnace. The melts were heated at 1510 °C with induction furnace, and then the alloying elements were added to the induction furnace. Pure cerium was inoculated to absorb the oxides of the alloy. The cerium

Table 1: Chemical composition of the test sample (wt.%).

Chemical composition (wt.%)					
Fe	C	Mn	Cr	P	Si
Bal.	2.05	0.30	11.50	0.01	0.25

content in S1–S19 samples was kept constant at 0.03 wt%. Y-block mold was made from chemically bonded sand using 1.5 wt% binder. Samples were casted into $10 \times 10 \times 10$ mm for experimental research. The process parameters used in the experimental studies are given in Table 2. Austempering was carried out in two stages. In the first stage, the samples were austenitized and in the second stage, the austenitized samples were austempered by isothermal annealing. The samples were austenitized at 1050 °C for 1 h, and then transferred to a constant temperature salt bath for austempering. After keeping at this temperature for 3, 6, 9, and 12 h, it was cooled to room temperature to complete the austempering process. Austenitizing was carried out in the furnace. Austempering was applied at different temperatures such as 550, 600, 650, and 700 °C.

The produced samples were ground and polished to determine the microstructural changes. Samples were etched in a solution containing 98 wt% ethanol and 2 wt% nitric acid. Microstructural differences of the samples were determined by scanning electron microscopy (SEM: ZEISS EVO LS10), energy dispersive spectroscopy (EDS), elemental mapping, X-ray diffraction (XRD: BRUKER) Cu/Kα ($\lambda = 1.54056$ Å) analysis. The microhardness measurements of the samples were made in the QNESS Q10 device with a 100 g load and a period of 15 s.

3 Results and discussion

3.1 Effect of Ce on microstructural assessments of samples

During confidential solidification, heat is transferred through the solid/liquid interface. The heat transfer from the interface to the solid should equalize between liquid/solid interface. A solid/liquid interface heading towards the supercooled liquid is unbalanced. Inoculation might create unstable flat eutectic fronts. The inoculation of Ce could occur "Ce_xO_yS" in a binary eutectic alloy [12–14]. The microstructure of the as-casted sample decomposed into coarse austenite dendrites with eutectic carbides (Figure 1a). Cerium was used as an inoculant in this research because it forms Ce_xO_yS with a crystallographic structure close to M_7C_3 carbide [14].

The effect of cerium on the microstructure of the samples is given in Figure 1b and c. As shown in Figure 1b, the eutectic structure was thinner and the chromium carbides were almost broken. The carbides occurred as eutectic chromium carbides at dendrite boundaries. The addition of cerium formed a eutectic structure with a finer eutectic carbide network that dissociated into chromium carbide. The dendrite arm spacing (DAS) and the diameter of the eutectic chromium carbides decreased. Also, the Ce addition of 0.09 wt% reduced the dendrite arm distance from 80 to
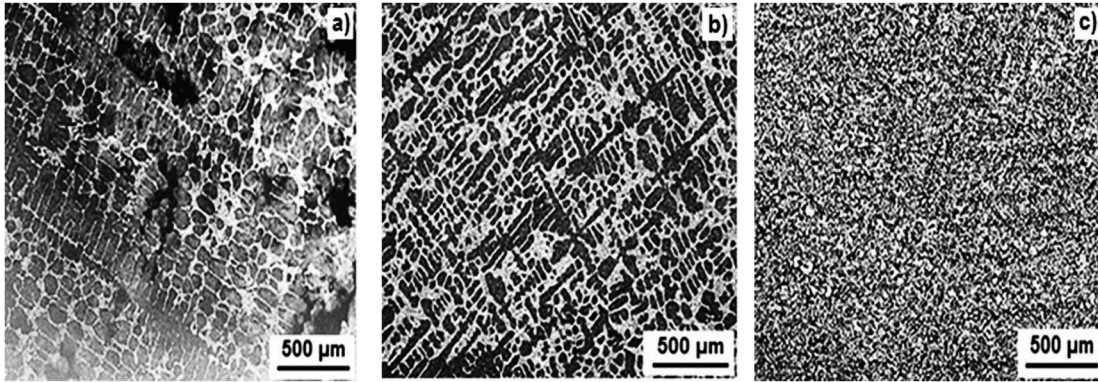
Table 2: Process parameters for experimental studies.

Sample no.	Destabilization temperature	Destabilization time	Quench medium	Subcritical diffusion temperature	Subcritical diffusion time	Quenching
S-Ref	As-casted	Unmodified				
S1a	As-casted	Modified by 0.03 wt.% Ce				
S1b	As-casted	Modified by 0.09 wt.% Ce				
S1	1050 °C	1 h	Salt	550	3 h	Air
S2	1050 °C	1 h	Salt	550	6 h	Air
S3	1050 °C	1 h	Salt	550	9 h	Air
S4	1050 °C	1 h	Salt	550	12 h	Air
S5	1050 °C	1 h	Salt	600	3 h	Air
S6	1050 °C	1 h	Salt	600	6 h	Air
S7	1050 °C	1 h	Salt	600	9 h	Air
S8	1050 °C	1 h	Salt	600	12 h	Air
S9	1050 °C	1 h	Salt	650	3 h	Air
S10	1050 °C	1 h	Salt	650	6 h	Air
S11	1050 °C	1 h	Salt	650	9 h	Air
S12	1050 °C	1 h	Salt	650	12 h	Air
S13	1050 °C	1 h	Salt	700	3 h	Air
S14	1050 °C	1 h	Salt	700	6 h	Air
S15	1050 °C	1 h	Salt	700	9 h	Air
S16	1050 °C	1 h	Salt	700	12 h	Air

Figure 1: Optical micrographs viewing the effect of the modifier on the structure and dispersion of eutectic carbides, a) unmodified sample, b) $S1_a$, c) $S1_b$.

40 μm. Increasing the Ce concentration to 0.03 wt% reduced the arm distance to 15 μm. Due to the partial and local solution of the eutectic chromium carbide, the size and rate of the eutectic carbide phase in the sample decreased after heat treatment.

Heat transfer through the Ce_xO_yS solid particles begins when solidification occurs. Theoretically, heat flow to the liquid would occur only when the liquid was cooled below T_m during the solidification process [12]. If nucleation occurs in Ce_xO_yS particles in the liquid, this may occur at the beginning of solidification. Since a certain degree of supercooling is required before nucleation occurs, the first solid Ce_xO_yS particles will become supercooled liquid and the latent heat of solidification will be transferred to the liquid [12–14]. The unique spherical Ce_xO_yS solid particles formed arms in many paths. As the primary arms lengthen, their surfaces became unstable. It is divided into secondary or tertiary arms. The SEM view of the (S1b) as-casted sample is illustrated in Figure 2. The as-casted sample

consisted of hard eutectic $(Fe,Cr)_7C_3$ carbides in austenite matrix. EDS spectrums and analysis of (S_{1b}) as-casted sample are displayed in Figure 3. The presence of Fe, C, Cr, Ce, Si, Mn elements was determined. The microstructure of S_{-Ref} showed the uneven distribution of large eutectic CrCs and stable dissolution of lesser globular secondary CrCs. The austempering process of the sample promoted the homogeneous dispersion of eutectic and secondary CrCs and reduced the dimension of the carbides.

Elemental mapping analysis of (S_{1b}) as-casted sample is depicted in Figure 4. White regions in the microstructure represented chromium carbides. Carbides, martensite, and retained austenite were the basic components. The martensite phase was seen as dark gray and retained austenite was light gray. The white regions consisted of cerium, sulfur, phosphorus, and oxygen. These regions appeared like cerium oxysulfide in which chromium carbide nucleated non-uniformly. The white regions in Figure 3b showed that Ce_xO_yS like Ce_2O_2S acted as a heterogeneous nucleus for eutectic
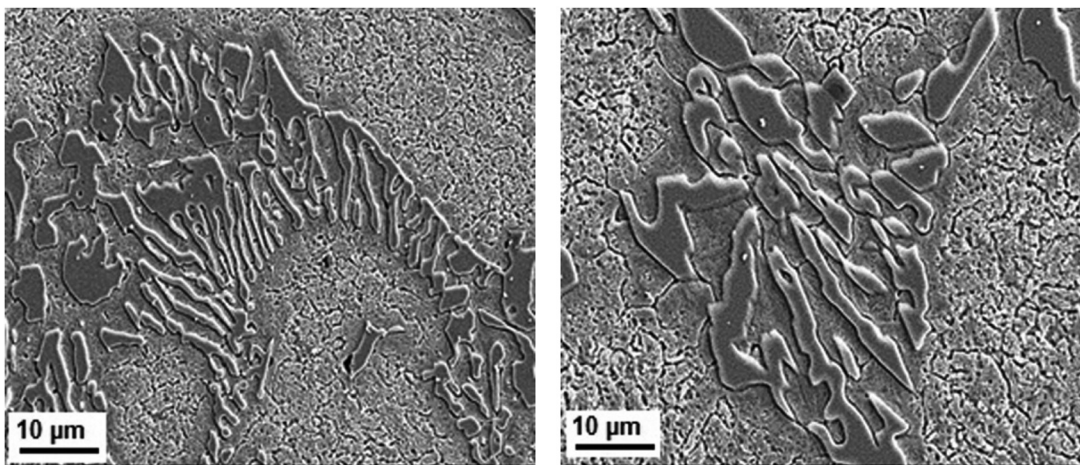

Figure 2: Scanning electron microscopy (SEM) micrographs of the as-casted sample.
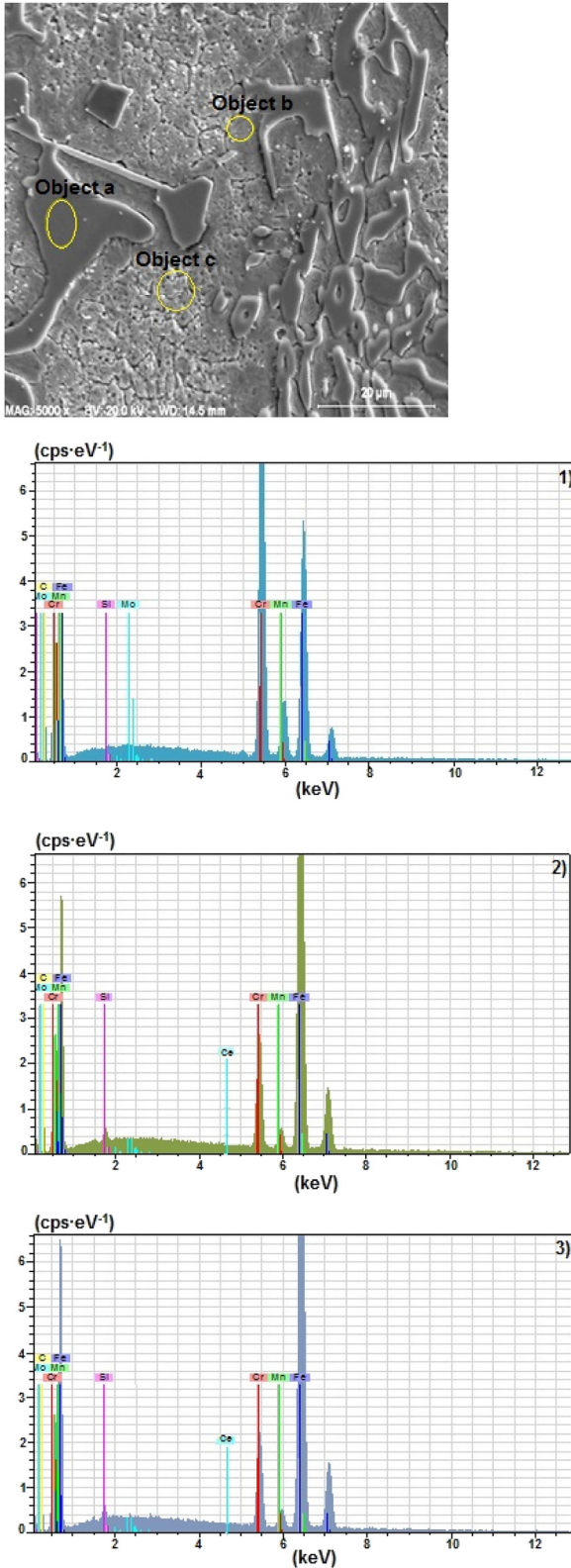
Figure 3: Energy dispersive spectroscopy (EDS) spectrums and analysis of S1$_b$ as-casted sample.

carbide. When the composition of the alloy deviated from the stable eutectic composition, solidification began near liquid temperature and, primary austenite dendrites occurred [12]. As the dendrite thicknesses dissolved, the alloy repelled the remaining liquid until the eutectic solidified. It consisted of pearlite, ferrite, and M_7C_3. The small phase then appeared as isolated pearlite islands. In some localized areas, the temperature gradient in the fluid rose above the critical temperature in the structure and the dendrite ends were reinforced by eutectic. The alloy solidifies 100% eutectic with the overall composition instead of the eutectic composition. A similar change can occur if the growth rate is increased above a critical level. In both cases, primary dendrites disappear because the eutectic can grow at a higher temperature than the ends of the dendrites [12].

The Ce_xO_yS (such as Ce_2O_2S) must meet two cases to become valid disparate nuclei [12–14]: a) the melting period of inclusions was higher than the eutectic temperature and b) the lattice mismatch between inclusions and eutectic carbides was small. Ce combines effectively with (S) and (O) and removes them from the melt. According to the Fe-C metallurgical, if (S) and (O) are removed and the solution is purified, the surface tension of the solution increases. This causes a rise in the nucleation free energy of the crystalline phase, which may require extra energy to occur nuclei [15]. Thus, crystal nucleation forms at low temperature, the liquid line drops along solidification, and the supercooling ratio of the eutectic reaction increases [15–18]. These factors led to changes in the microstructure of tool steels. Figure 4 shows the volume rate of carbides in different austenitizing temperatures. Chromium carbide dissolved in austenite gradually as the temperature and time increase during the austenitization process. As the temperature increased, the proportion of retained carbides decreased. Also, unsolvable carbides can hinder grain growth of alloy at high temperatures [17–20]. The crystalline solid solution of the ferrite and austenite contains a certain amount of alloying elements. When steel is cooled at high temperatures, austenite separates into ferrite and cementite. The existence of elements in austenite can delay eutectoid conversion. Several phases were semi-stable at room temperature because cold work tool steel contained a large amount of carbon. The matrix of the samples was a solid solution of Cr and C in α-Fe. Chromium was the main carbide occurring elements of M_7C_3. The smaller the size of the eutectic carbide, the larger the interface between matrix and carbides. Therefore, the eutectic carbides dissolved during annealing tend to increase. The proportion of elements (Cr and C) in austenite increased
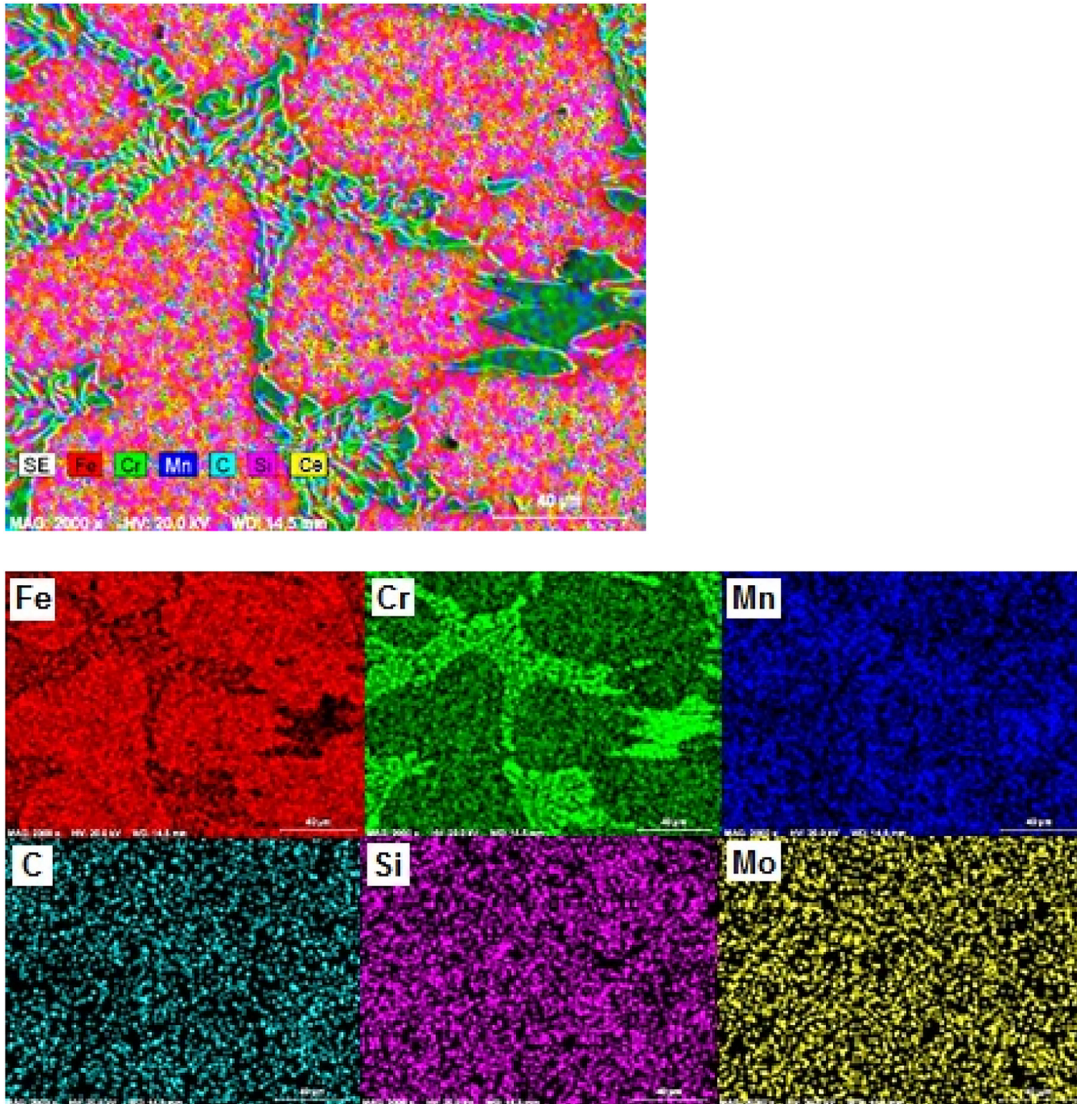
Figure 4: Elemental mapping analysis of S1$_b$ as-casted sample.

along the annealing procedure. The resolution of elements in austenite reduced with decreasing temperature. Subsequently, the austenite phase was separated into carbides. Homogeneous dispersion of fine carbides in the matrix resulted in uniform hardness of the alloy. The 1050 °C process helped dissolve most carbides. The austenitization temperature decreased in carbide volume at 1050 °C. At 1050 °C, the dimension and amount of undissolved carbides are decreased. The austenitizing temperature of 1050 °C led to an increase in the grain size of the previous austenite, which preserved the austenite content and increased delta ferrite.

Figure 5 represents the effect of different austempering temperatures on the microstructure. Two phases were identified in the matrix of the austempered sample. Dark colored bainite and ferrite were detected in the form of needles. The orientation of bainite laths at low conversion temperature was irregular and thinner. In the first phase of transformation, bainite nucleated at the austenite grain boundaries, refused to convert carbon to austenite, and expanded in parallel plates or laths. Therefore, bainite and less retained austenite were observed in the microstructure of the sample. Some acicular ferrite was also observed at higher annealing temperatures. The average length of the laths and the pointed ferrite was the same, but their thickness was different. The shape of the bainite in the early stage of transformation was very sharp and took the form of a lath due to lateral growth. According to the microstructural changes, the austenite annealing temperature and the bainite length changed very little and the bainite width had a significant difference. X-ray diffraction

analysis of the S_{1b} and S_5 samples consisted of Cr_7C_3, (α) ferrite, (γ) austenite in Figures 6 and 7.

During the annealing process, the properties of the material improved, but the austenite crystal structure remained unchanged and was soft. After the austenite annealing process was applied, the austenite was permanently transformed into martensite structure, which represented the permanent change in the microstructure. The
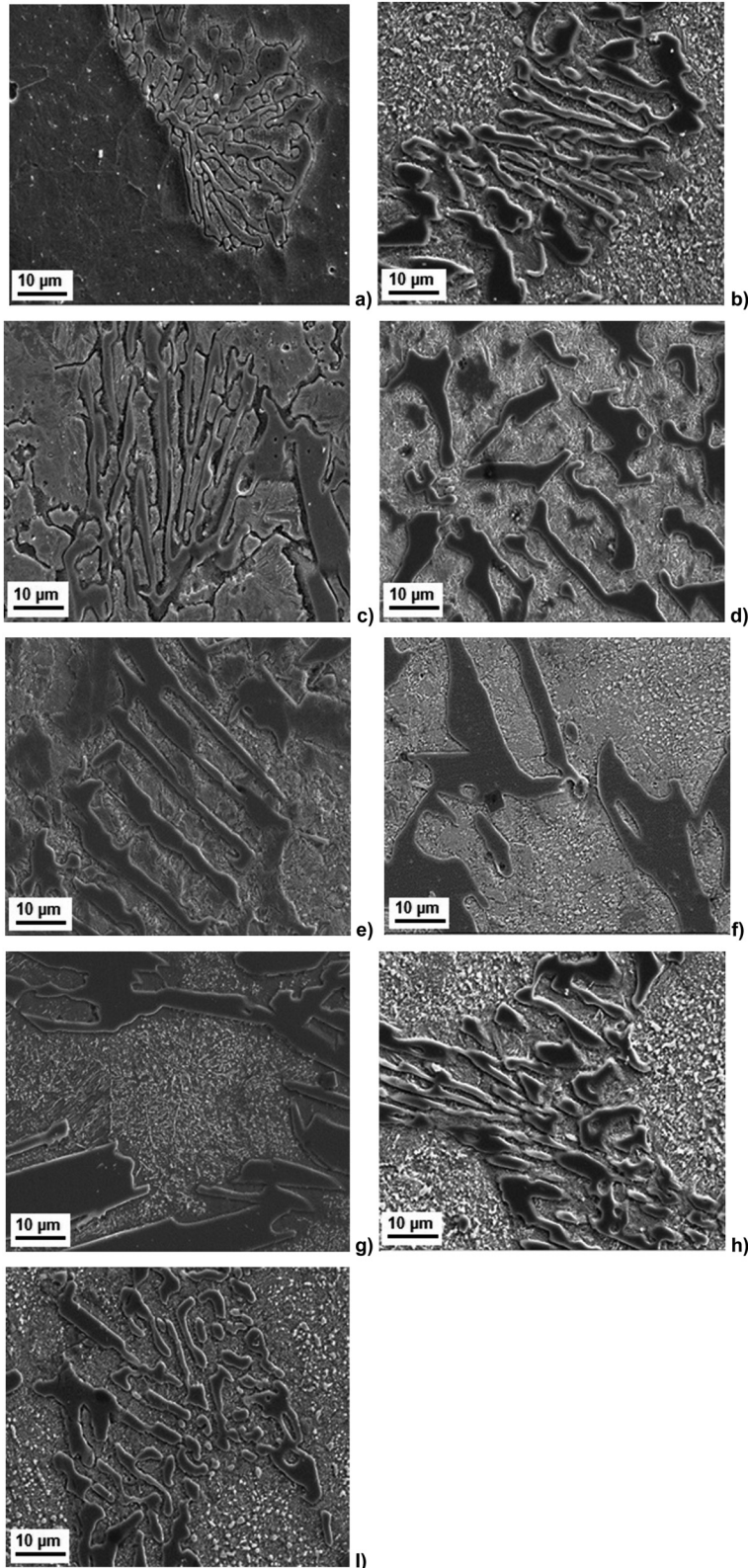
Figure 5: Scanning electron microscopy (SEM) micrographs of the experimental samples, a) S_2, b) S_3, c) S_{10}, d) S_{11}, e) S_{14}, f) S_{15} g) S_{17}, h) S_{18}, i) S_{19}.
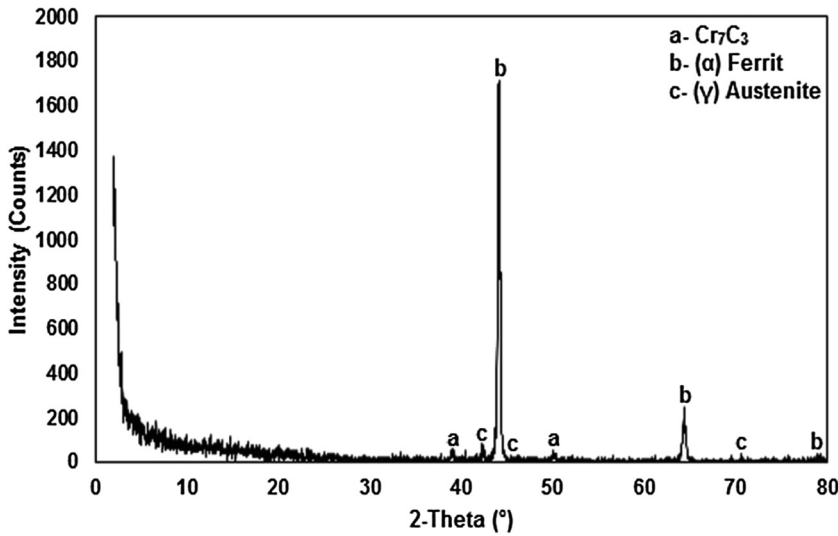
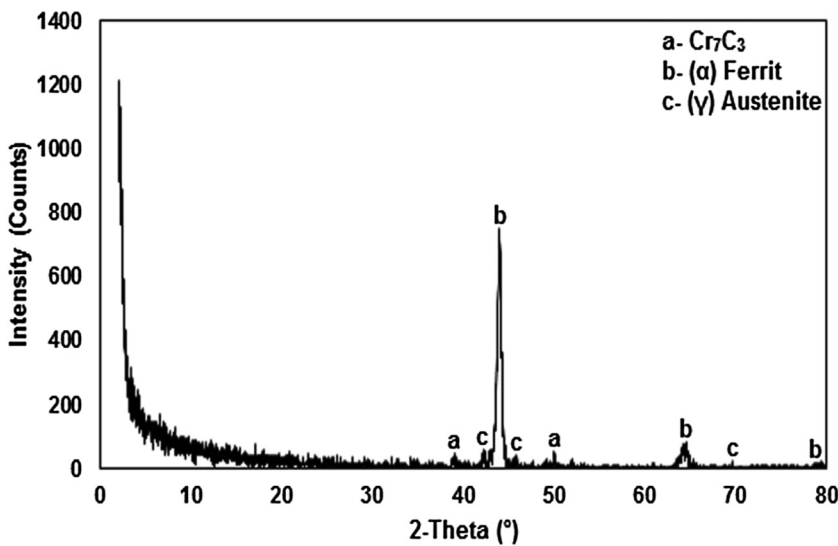**Figure 6:** X-ray diffraction (XRD) analysis of S_{1b} as-casted sample.

Figure 7: X-ray diffraction (XRD) analysis of S_5 sample.

remaining austenite was soft in nature. This shortens the life of the tool and becomes martensite during operation, but it was fragile in nature. The higher the austenitizing temperature, the dissolving most of the excess carbides in the austenite before quenching decreased the *M* value. The lower the Ms, the higher the retained austenite rate. Therefore, the retained austenite rate was higher during quenching at 1150 °C. Austempering treatment was an effective method of reducing retained austenite. The higher the austenitizing temperature, the more evident the influence.

3.2 Hardness

Microhardness distributions of the samples are depicted in Figure 8. The increase in austenitizing temperature caused an increase in hardness, but at a higher temperature, the amount of austenite retained in the structure increased, resulting in a decrease in hardness. After austempering, the peak hardness was increased and occurred at a higher austenitizing temperature. Maximum hardness was achieved when all remaining austenite was converted to martensite. The cooling rate increased the hardness (Figure 8a). The hardness only rose at 1000 °C and then dropped above this temperature. The formation of martensite, which contained higher unsolved Cr and C, might be caused for the increased rigidity. A decrease in hardness above 1000 °C will cause an increase in the ratio of the retained austenite due to the increase in chromium ratio in the matrix and the decrease in Ms temperature. Increasing the austenitizing time reduced hardness at any temperature. This was believed to be due to the retained
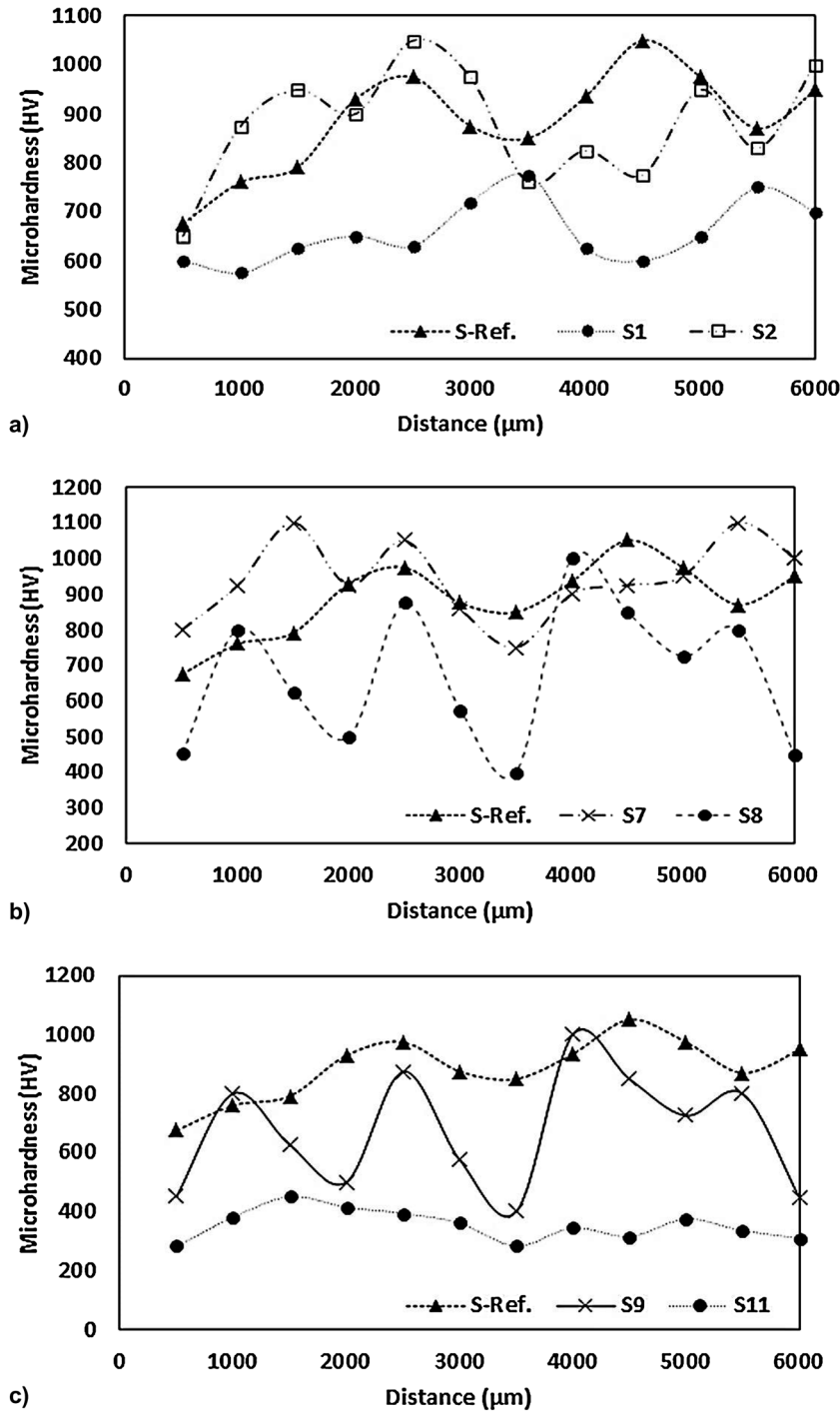
a)

b)

c)

Figure 8: Microhardness distributions of test samples dependent on a) cooling rate, b) austempering temperature, c) austempering time.

austenite. The hardness of low temperature tempered austenite was higher than that of high temperature tempered austenite. The increase in hardness with the austempering process was due to the crystallographic and microstructural changes and fine dispersion of micro carbides. The increase of austempering temperature decreased hardness and homogeneity of microstructure (Figure 8b). Another feature was that the precipitation of carbide particles depends on the duration of the process, and the formation of these time-varying nano-carbide particles helped to improve the mechanical properties of cold work tool steels after austempering treatment. The higher the proportion of carbon in the composition, the higher the hardness due to the finer carbides formed. The austenite annealing process was the cause of carbide nucleation and consequently lowers the formation temperature of fine carbides. As the annealing temperature increased, the hardness decreased, but the wear resistance and impact energy improve [21]. The

presence of Ce helped to create a more pronounced secondary hardening peak and provided higher working hardness. It offers a better annealing resistance for standard austenitizing temperatures of 1050 ℃. The low austempering time increased the homogeneity of microstructure and hardness.

4 Conclusions

The important results of this research are as follows:

The addition of cerium to X210Cr12 tool steel enhanced nucleation and refining of eutectic carbides.

The austempering treatment increased the hardness of the cold work tool steel by reducing the retained austenite.

After austenitization at 1050 ℃, the amount of undissolved carbides was very small. It was impossible to prevent the growth of grains during the second stage austenitization at 1050 ℃, and fine carbides formed along the boundary and in martensite.

The austempering process provided the best balance between carbide solution and grain expansion.

At 1050 ℃, more carbide dissolved, and the matrix was rich in carbon and alloying elements.

After the Ce inoculation, there was a significant difference in the magnitude and distribution of the eutectic carbides. M_7C_3 eutectic carbide was refined and dispersed.

CeOS inclusions could be used to increase nucleation and develop refining of eutectic carbides.

References

[1] A. Molinari, M. Pellizzari, S. Gialanella, G. Straffelini, and K. H. Stiasny, "Effect of deep cryogenic treatment on the mechanical properties of tool steels," *J. Mater. Process. Technol.*, vol. 118, nos. 1–3, pp. 350–355, 2001, https://doi.org/10.1016/S0924-0136(01)00973-6.

[2] J. Y. Huang, Y. T. Zhu, X. Z. Liao, I. J. Beyerlein, M. A. Bourke, and T. E. Mitchell, "Microstructure of cryogenic treated M2 tool steel," *Mater. Sci. Eng.*, vol. 339, nos. 1–2, pp. 241–244, 2003, https://doi.org/10.1016/S0921-5093(02)00165-X.

[3] A. Kokosza and J. Pacyna, "Evaluation of retained austenite stability in heat treated cold work tool steel," *J. Mater. Process. Technol.*, vol. 162, no. 163, pp. 327–331, 2005, https://doi.org/10.1016/j.jmatprotec.2005.02.068.

[4] T. Večko Pirtovšek, G. Kugler, M. Godec, and M. Terčelj, "Microstructural characterization during the hot deformation of 1.17C–11.3Cr–1.48V–2.24W–1.35Mo ledeburitic tool steel," *Mater. Char.*, vol. 62, no. 2, pp. 189–197, 2011, https://doi.org/10.1016/j.matchar.2010.11.016.

[5] V. Firouzdor, E. Nejati, and F. Khomamizaheh, "Effect of deep cryogenic treatment on wear resistance and tool life of M2 HSS drill," *J. Mater. Process. Technol.*, vol. 206, nos. 1–3, pp. 467–472, 2008, https://doi.org/10.1016/j.jmatprotec.2007.12.072.

[6] A. Akhbarizadeh, A. M. A. Shafyei, and M. A. Golozar, "Effects of cryogenic treatment on wear behaviour of D6 tool steel," *Mater. Des.*, vol. 30, no. 8, pp. 3259–3264, 2009, https://doi.org/10.1016/j.matdes.2008.11.016.

[7] N. B. Dhokey and S. Nirbhavane, "Dry sliding wear of cryo-treated multiple tempered D3 tool steel," *J. Mater. Process. Technol.*, vol. 209, no. 3, pp. 1484–1490, 2009, https://doi.org/10.1016/j.jmatprotec.2008.03.069.

[8] S. S. Grill, J. Singh, R. Sigh, and H. Sigh, "Metallurgical principals of cryogenically treated tool steels – a review on the current state of science," *Int. J. Adv. Manuf. Technol.*, vol. 54, pp. 59–82, 2011, https://doi.org/10.1007/s00170-010-2935-5.

[9] Ö. M. Murathan, K. Davut, and V. Kilicli, "Effect of austenitizing temperatures on the microstructure and mechanical properties of AISI 9254 steel," *Mater. Test.*, vol. 63, no. 1, pp. 48–54, 2021, https://doi.org/10.1515/mt-2020-0007.

[10] C. H. Surberg, P. F. Stratton, and K. Lingenhole, "The effect of cryogenic treatment on the properties of AISI D2," *Mater. Manuf. Process.*, vol. 24, nos 7–8, pp. 863–867, 2009, https://doi.org/10.1080/10426910902917421.

[11] A. Oppenkowski, S. Weber, and W. Theisen, "Evaluation of factors influencing deep cryogenic treatment that affect the properties of tool steels," *J. Mater. Process. Technol.*, vol. 210, no. 14, pp. 1949–1955, 2010, https://doi.org/10.1016/j.jmatprotec.2010.07.007.

[12] X. Chen and Y. Li, "Fracture toughness improvement of austempered high silicon steel by titanium, vanadium and rare earth elements modification," *Mater. Sci. Eng.*, vol. 444, nos. 1–2, pp. 298–305, 2007, https://doi.org/10.1016/j.msea.2006.08.113.

[13] Y. Qu, J. Xing, X. Zhi, J. Peng, and H. Fu, "Effect of cerium on the as-casted microstructure of a hypereutectic high chromium cast iron," *Mater. Lett.*, vol. 62, nos. 17–18, pp. 3024–3027, 2008, https://doi.org/10.1016/j.matlet.2008.01.129.

[14] K. Amini, S. Nategh, and A . Shafyei, "Influence of different cryotreatments on tribological behavior of 80CrMo12 5 cold work tool steel," *Mater. Des.*, vol. 3, no. 10, pp. 4666–4675, 2010, https://doi.org/10.1016/j.matdes.2010.05.028.

[15] Y. M. Rhyim, S. H. Han, Y. S. Na, and J. H. Lee, "Effect of deep cryogenic treatment on carbide precipitation and mechanical properties of tool steel," *Solid State Phenom.*, vol. 118, pp. 9–14, 2006, https://doi.org/10.1016/j.matlet.2008.01.129.

[16] D. Das, A. K. Dutta, V. Toppo, and K. K. Ray, "Effect of deep cryogenic treatment on the carbide precipitation and tribological

behavior of D2 steel," *Mater. Manuf. Process.*, vol. 22, no. 4, pp. 474–480, 2007, https://doi.org/10.1080/10426910701235934.

[17] T. Teker, I. S. Dalmış, and R. Yılmaz, "Effect of heat treatment on wear behavior of GX200Cr13Ni6WMoMn," *Mater. Test.*, vol. 61, no. 5, pp. 441–447, 2019, https://doi.org/10.3139/120.111339.

[18] D. Mohan Lal, S. Renganarayanan, and A. Kalanidhi, "Cryogenic treatments to augment wear resistance of tool and die steels," *Cryogenics*, vol. 41, no. 3, pp. 149–155, 2001, https://doi.org/10.1016/S0011-2275(01)00065-0.

[19] K. D. Timmerhaus and R. P. Reed, *Cryogenic Engineering*, New York, USA, Springer, 2007, pp. 3–37.

[20] V. Leskovsek, M. Kalin, and J. Vizintin, "Influence of deep cryogenic treatment on wear resistance of vacuum heat-treated HSS," *Vacuum*, vol. 80, no. 6, pp. 507–518, 2006, https://doi.org/10.1016/j.vacuum.2005.08.023.

[21] T. Engelke and A. Esderts, "Analytical strength assessments of austempered ductile iron components," *Mater. Test.*, vol. 60, no. 10, pp. 940–944, 2018, https://doi.org/10.3139/120.111235.

The authors of this contribution

Tanju Teker
Tanju Teker born in Sivas in 1971, works in the University of Sivas Cumhuriyet, Faculty of Technology, Department of Manufacturing Engineering, Sivas, Turkey. He graduated in Metallurgy Education from Gazi University, Ankara, Turkey, in 1997. He received his MSc and PhD degrees from Firat University, Elazig, Turkey in 2004 and 2010, respectively. His research interests are metal coating techniques, casting, fusion, and solid-state welding methods.

S. Osman Yilmaz
S. Osman Yilmaz born in Elazig in 1966, works at the University of Namık Kemal, Faculty of Engineering, Department of Mechanical Engineering, Corlu, Tekirdağ, Turkey. He received his BSc from METU University, Ankara, Faculty of Engineering, Metallurgy and Materials Engineering Department in 1989, his MSc from the Institute of Science and Technology, Metallurgy Department in 1992, and his PhD from the University of Firat, Institute of Science and Technology, Metallurgy Department, Elazig in 1998. He studied metal coating techniques, surface modification, welding, casting, and wear.

S. Özmen Eruslu
S. Özmen Eruslu born in 1977, works at the University of Namık Kemal, Faculty of Engineering, Department of Mechanical Engineering, Corlu, Tekirdağ, Turkey. He graduated in Mechanical Engineering from Süleyman Demirel University, Isparta, Turkey, in 1999. He received his MSc and PhD degrees from Trakya University, Edirne, Turkey and Dokuz Eylül University, İzmir, Turkey in 2002 and 2008, respectively. His research interests are material design and behaviors, finite element analysis, and composite materials.